Extended Abstracts of the 2020 International Conference on Solid State Devices and Materials, VIRTUAL conference, 2020, pp583-584

Highly Sensitive p-GaAsSb/n-InAs Nanowire Backward Diodes with 2.2 MV/W for Low Power Microwave Harvesting

Tsuyoshi Takahashi[1,2], Kenichi Kawaguchi[1,2], Masaru Sato[1,2], Michihiko Suhara[3], and Naoya Okamoto[1,2]

[1] Fujitsu Laboratories Ltd.
10-1 Morinosato-Wakamiya, Atsugi, Kanagawa 243-0197, Japan
Phone: +81-46-250-8238, E-mail: takahashi.tsuyo@fujitsu.com
[2] Fujitsu Limited
10-1 Morinosato-Wakamiya, Atsugi, Kanagawa 243-0197, Japan
Phone: +81-46-250-8238
[3] Tokyo Metropolitan University
1-1 Minami-Osawa, Hachioji, Tokyo 192-0397, Japan
Phone: +81-42-677-2765

Abstract

Highly sensitive nanowire backward diodes (NW BWDs) with 2.2 MV/W, which are more advanced than conventional well-designed Schottky barrier diodes, were developed using a p-$GaAs_{0.4}Sb_{0.6}$/n-InAs tunnel junction structure for low-power microwave harvesting at zero bias. A large dynamic range of values in detected voltage was obtained when a side face of the top region of NW-BWD contacted to an anode. Device simulations clarified that carrier depletion improved the forward breakdown voltage (BV) of the NW BWDs.

1. Introduction

Batteryless systems are required to solve the demand for maintenance-free Internet of things (IoT) sensors. Some types of ambient energy harvesting technologies have been planned to supply DC power to operate IoT sensors. The ambient RF energy harvesting is an efficient candidate because RF power can be obtained anywhere using wireless radio communications, such as wireless local area networks (LANs). Schottky barrier diodes (SBDs) are generally used as RF-to-DC energy converters in ambient RF energy harvesting. The conventional SBDs are not efficient to rectify the low input of RF power (P_{in}), which is less than 1 μW, owing to their low sensitivity at around zero bias. To solve this problem, the use of backward diodes (BWDs), which are based on the sharp rectification provided by interband tunneling, has been proposed [1]. As scaling of the junction should improve the sensitivity, nanowire (NW) structure was introduced to form a small junction of less than 200 nm [2]. In this study, although the P_{in} was much less than 1 μW, the sensitivity of the p-GaAsSb/n-InAs NW BWD was extended up to 2.2 MV/W, which is more than that of the conventional SBDs, at 2.4 GHz under a zero bias. Moreover, the dynamic range in the V_{det} was improved by adopting a carrier-depletion structure at the top of the NW BWD.

2. Device Fabrication

For the NW BWD growth, the selective-area epitaxial growth and vapor–liquid–solid (VLS) growth methods were applied. Each NW position was defined by an electron-beam lithographic technique followed by the formation of Au catalysts in a SiN dielectric film. The p-$GaAs_{0.4}Sb_{0.6}$/n-InAs NW-BWD segments were grown by the VLS growth method using Au catalysts. The energy band diagram of NW BWD under equilibrium condition is shown in Fig. 1(a). An n-GaAs epitaxial layer was formed to stabilize the NW growth on a 3-inch semi-insulated GaAs(111)B substrate prior to NW BWD growth. A cross-sectional diagram of the fabricated p-GaAsSb/n-InAs NW BWD is shown in Fig. 1(b). The surface was fully passivated with a thin 14 nm AlO_x film by atomic layer deposition after the growth of the NW BWDs. The NW BWDs were embedded in a 1.5 μm-thick spin coated benzocyclobutene (BCB) to form the interlayer film. A Pt-based anode was formed on the top of the GaAsSb segments. In this study, a design of reduction in parasitic capacitance that is brought by the interconnection layout, was employed to obtain high frequency operations. A small anode pad of area 20 × 50 μm^2 was introduced.

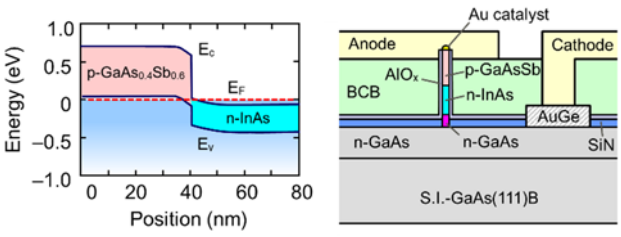

(a) (b)

Fig. 1 (a) Energy band diagram of a p-$GaAs_{0.4}Sb_{0.6}$/n-InAs NW BWD under equilibrium condition, and (b) cross-sectional diagram of the NW BWD after an interconnection.

3. Experimental Results

A SEM image of the grown NW BWDs is shown in Fig. 2(a). Figure 2(b) shows the normalized *I–V* characteristics of the fabricated NW BWDs when a single nanowire number was performed. Although the reverse current was almost identical, two types of *I–V* characteristics were obtained as different forward break down voltage (BV). The device simulation was performed to clarify the difference in VBs. Figure

3(a) shows that two types of BWD structures were used in the simulations. The main difference between them was extended anode length. Type A has an anode just on the top of the NW. Type B has an extended anode, consisting of an metal-oxide-semiconductor (MOS) structure, with a length (L) of 0.4 μm at the side face of the NW in addition to the top contact. Device simulations were performed using these structure models. Although the reverse current was identical for the calculated I–V characteristics, different forward current was obtained as shown in Fig. 3(b). The BWD with higher BV (type 2 in Fig. 2) had an extended anode structure like type B BWD. As a result, forward current decreased due to the formation of depletion layer in the NWs [3]. Meanwhile, the anode of the other BWD (type 1 in Fig. 2) contacted only the top of the NW, as shown in type A of Fig. 3.

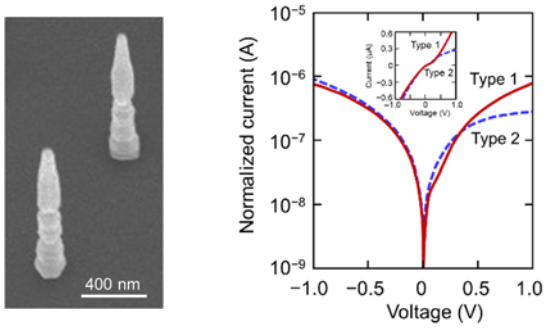

(a) (b)

Fig. 2 (a) A SEM image of NW BWDs. (b) Two types of normalized logarithmic I–V characteristics of the fabricated NW BWDs. Inset shows the linear I–V characteristics.

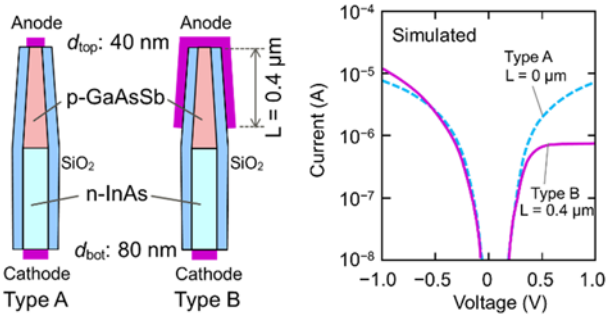

(a) (b)

Fig. 3 (a) Device structures adopted for device simulation. Extended anode length on the side face of the NW is different. (b) The I–V characteristics that were calculated by using a device simulator.

The microwave-detection measurements under low microwave input power were performed using two types of NW BWDs. Figure 4 shows the detected voltage (V_{det}) and impedance-matched voltage sensitivity ($\beta_{v,opt}$) as a function of input power (P_{in}) at 2.4 GHz under zero bias. Both NW BWDs displayed dependence on linear V_{det} even though P_{in} was as low as −50 dBm. Type 2 NW BWD has large dynamic range than type 1 because type 2 NW BWD has a large forward BV. Alternatively, dynamic range of type 1 NW BWD was limited from −70 dBm to −50 dBm due to a small forward BV. Both NW BWDs showed much higher sensitivities than the sensitivity of 62 kV/W for SBDs [4]. Especially, the type-1 NW BWD achieved a large $\beta_{v,opt}$ of 2.2 MV/W and it was three times higher than the previous reports [5]. The high sensitivity was primarily due to the low capacitance by employing the NW structure and the small anode pad. Since, obtaining high sensitivity is more effective to obtain high power conversion efficiency (PCE) from environmental microwave, highly sensitive nanowire BWDs are considered to be very effective for ambient RF energy harvesting. The slightly lower sensitivity of type-2 NW BWD was considered to be caused by higher series resistance from enhanced carrier depletion in p-GaAsSb segment. The realization of high BV and low series resistance will improve both dynamic range and sensitivity of the NW BWDs.

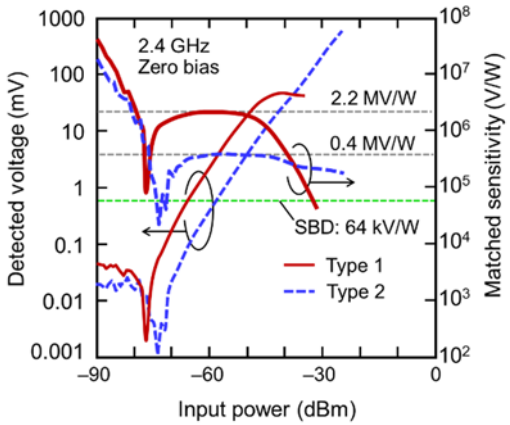

Fig. 4 Detected voltage and impedance-matched voltage sensitivities for type 1 and type 2 NW BWDs as a function of the input power at 2.4 GHz under zero bias.

4. Conclusions

A large microwave sensitivity of 2.2 MV/W, which exceeded that of well-designed SBDs, was achieved using p-$GaAs_{0.4}Sb_{0.6}$/n-InAs NW BWD for ambient RF energy harvesting at zero bias. When an extended anode contacts to a side face of the NW BWD to form an MOS structure, a large dynamic range of values in detected voltage was obtained.

Acknowledgements

The authors would like to thank Kozo Makiyama, Junko Hara, Kenji Saito and Yukio Ito for their technical support, and Takayuki Fujiwara and Shirou Ozaki for their helpful advice. This work was partly supported by JST CREST Grant Number JPMJCR16Q3, Japan.

References

[1] T. Takahashi *et al.*, IEEE Trans. Electron Devices, **62** (2015).
[2] T. Takahashi *et al.*, Appl. Phys. Express, **12**, 106502 (2019).
[3] T. Takahashi *et al.*, Jpn. J. Appl. Phys. **59**, SGGH03 (2020).
[4] C. Lorenz *et al.*, IEEE Trans. Microw. Theory Techn. 63, 4544.
[5] T. Takahashi *et al.*, Proc. ESSDERC2019, 214.